Available online at www.sciencedirect.com

SciVerse ScienceDirect

Procedia CIRP 3 (2012) 335 – 339

www.elsevier.com/locate/procedia

45th CIRP Conference on Manufacturing Systems 2012

Preliminary Study on Chemical Figuring and Finishing of Sintered SiC Substrate Using Atmospheric Pressure Plasma

K. Yamamura[a,]*, Y. Yamamoto[a], H. Deng[a]

[a]*Research center for ultra-precision science and technology, Graduate school of engineering, Osaka University, 2-1 Yamadaoka, Suita, Osaka 565-0871, Japan*

* Corresponding author. Tel.:+81-6-6879-7293 .*E-mail address*: yamamura@upst.eng.osaka-u.ac.jp

Abstract

Chemical figuring and finishing techniques using atmospheric pressure plasma were proposed for realizing damage free processing of a reaction sintered SiC substrate. Open-air type plasma chemical vaporization machining (PCVM) utilizing He based CF_4/O_2 mixture process gas demonstrated good linearity of the relationship between removal volume and plasma irradiation time which required in numerically controlled figuring. However, the surface roughness of the substrate processed by PCVM increased with an increase in removal depth by forming pores on the surface because etching rate of residual Si was about 3 times greater than that of SiC.

Keywords: Plasma CVM; Sintered SiC; Figuring

1. Introduction

Silicon carbide (SiC) is a promising next-generation semiconductor and structural material because of its excellent electrical, chemical, thermal and mechanical properties. With different manufacturing technologies, different types of SiC are obtained, such as single-crystal SiC grown by a modified Lely method, polycrystalline SiC prepared by chemical vapor deposition (CVD) and sintered SiC. In particular, reaction-sintered (RS) SiC shows many excellent properties, such as high bending strength and high thermal conductivity, compared with conventionally sintered SiC [1]. These properties make RS-SiC one of the most attractive materials for a glass lens mold, equipment parts for the fabrication of semiconductor devices, and a lightweight space telescope mirror substrate. However, it is difficult to achieve nanometric level form accuracy with a high integrity surface for RS-SiC because of its high hardness and chemical inertness. Chemical mechanical polishing (CMP) is now widely used as a finishing process for the surfaces of single-crystal SiC [2]. However, this technique is focused on the finishing of single-crystal SiC, and the material removal rate of CMP, which is reported to be less than 0.5 μm/h, is very low. Although a high rate of mechanical polishing with a hard abrasive, such as diamond, is achieved, microscratches and subsurface damage are inevitably introduced. Recently, hybrid CMP process, which uses a mixed abrasive slurry (MAS) composed of a mixture of colloidal silica slurry and nano-diamond abrasive, to increase the MRR keeping a defect-free surface [3-4].

To resolve the above issues, we proposed combined fabrication process consist of plasma chemical vaporization machining (PCVM) and plasma assisted polishing (PAP) for efficient high-precision figuring of RS-SiC material. PCVM is chemical figuring technique using atmospheric pressure plasma containing fluorine radical [5-6], and PAP is polishing technique combined with an irradiation of atmospheric pressure water vapor plasma for modification of the surface [7-10]. The aim of this study is evaluation of the removal properties of both plasma CVM and PAP for the RS-SiC substrate,

doi:10.1016/j.procir.2012.07.058

and is consideration of the feasibility as the efficient figuring process of precise molding or optical device.

In this paper, we report the removal characteristics of PCVM for RS-SiC substrate, such as the material removal rate (MRR), surface roughness, and surface morphology.

2. Experimental setup

Fig. 1 shows the schematic diagram of the NC-PCVM system. Electrode unit for generating plasma is constructed from coaxially arranged metal electrode and alumina ceramic tube. Diameter and material of the electrode are 3 mm and aluminum alloy, respectively. Composition and flow rate of the process gas is controlled by mass flow controller. Supplying of the gas from circumference of the tip of the electrode replaces the air to the process gas, and enables generating the plasma stably in the atmospheric pressure environment as shown in the Fig. 2. The applied high frequency electric field (f=13.56 MHz) generates the plasma in the narrow gap between the electrode and the substrate, and the typical gap distance is ranging from 0.1 to 0.5 mm.

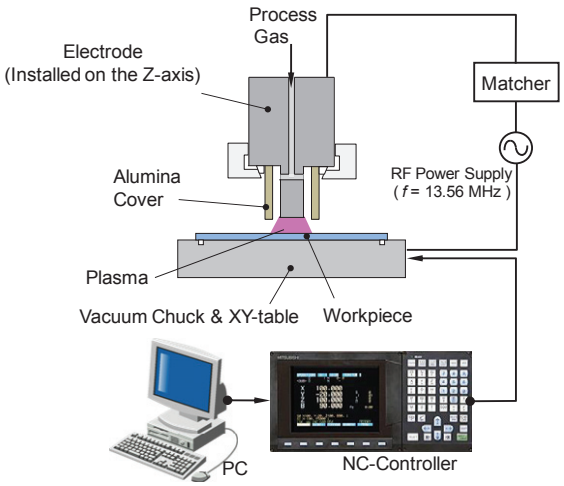

Fig. 1. Schematic diagram of the NC-PCVM system

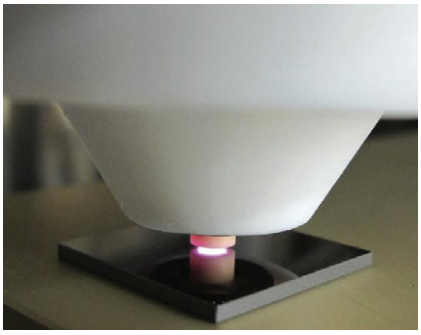

Fig. 2. Photograph of electrode unit and workpiece

Generated plasma region is localized in the vicinity of the electrode, because the mean free path of gas molecules is very small in atmospheric pressure condition. Therefore, figuring and patterning without masking are easily realized by scanning the localized reactive area. Workpiece is held by a vacuum chuck installed on the XY-table. Relative position and speed between the electrode and the workpiece are controlled by XY-table and Z-axis driven by AC servo motors. Strokes of the XY-table and Z-axis, and maximum scanning speed of the XY-table are ±300 mm, ±10 mm and 8000 mm/min, respectively. We use $He/CF_4/O_2$ mixture as reactive gas to generate fluorine radicals which react with RS-SiC including SiC phase, residual Si and residual C. Those elements are removed from the surface as volatile components such as SiF_4, CF_4 and CO_2. The local removal volume at a certain position on the workpiece can be controlled using the dwelling time of the electrode in XY-table scanning. The removal volume distribution on the workpiece is determined by the convolution of the removal function, which defined by removal footprint formed in an unit time, and the dwelling time distribution of the localized plasma. In the practical figuring process, the dwelling time distribution calculated by the deconvolution simulation of the removal volume distribution and the removal function determines the scanning speed distribution of the worktable. Numerically controlled scanning is performed by raster scanning, and then designed shape is obtained deterministically.

In this system, there is no gas evacuating process which needs expensive vacuum system, so that processing time and initial cost of the machine can be drastically reduced.

3. Results and discussion

3.1. Material removal rate

Material removal rates of RS-SiC were evaluated by using a scanning white light interferometer (SWLI) (Zygo, NewView 200CHR). Fig. 3 shows typical removal footprint formed by irradiation of fluorine contained atmospheric pressure plasma.

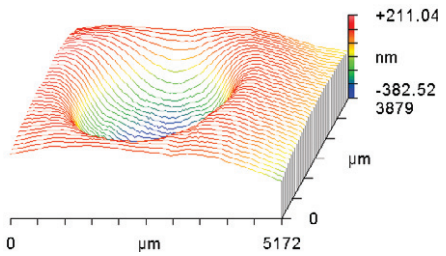

Fig. 3. Typical shape of the removal footprint (Power: 110 W, Flow rate: $He:CF_4:O_2$=750:10:10 sccm, Gap: 500 μm)

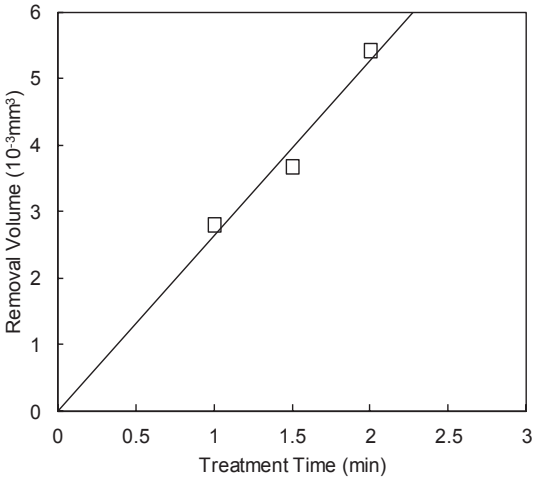

Fig. 4. Relationship between material removal volume and plasma irradiation time (Power: 100 W, Flow rate: He:CF_4:O_2=750:5:5 sccm, Gap: 500 μm)

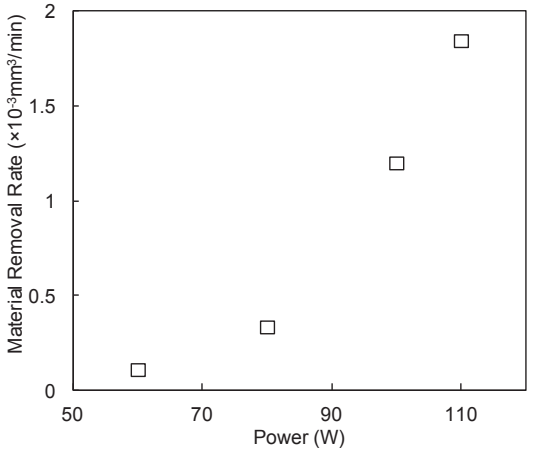

Fig. 5. Relationship between MRR and supplied electric power (Flow rate: He:CF_4:O_2=750:10:10 sccm, Gap: 500 μm)

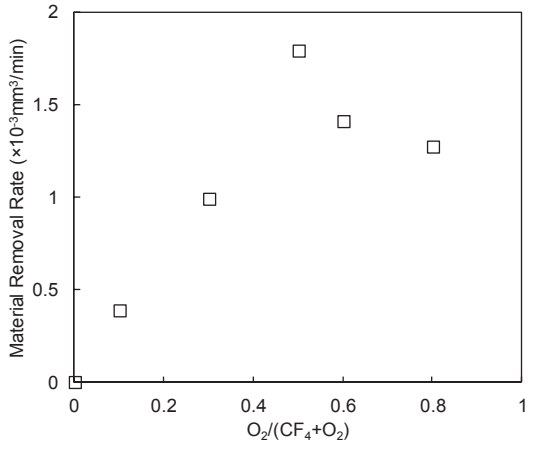

Fig. 6. Relationship between MRR and O_2/(O_2+CF_4) ratio (Power: 100 W, Flow rate: He:CF_4+O_2=750:20 sccm, Gap: 500 μm)

Removal footprint has an axisymmetric shape with a diameter of ca. 3.5 mm. We evaluated spatial resolution of the obtained footprint in figure correction by simulation which is based on the convolution model. Simulation result indicates that minimum correctable spatial wave length is 3 mm.

Fig. 4 shows relationship between material removal volume and plasma irradiation time. Removal volume linearly increased with an increase in plasma irradiation time.

Above two results indicate that NC-PCVM enables us to figure the objective shape for RS-SiC substrate with a spatial resolution of millimetre level by controlling the scanning speed of the worktable, which determines dwell time of plasma.

Fig. 5 shows relationship between MRR and applied electric power. MRR increased nonlinearly with an increase in electric power. In the case of high electric power condition, surface temperature increased due to the heat flow from plasma, and it is assumed that rise of surface temperature resulted in drastic increase of MRRby promoting chemical reaction between the reactive species and the surface atoms. If the supplied electric power exceeds 110 W, glow-to-arc transition occurs. In this work, supplied power was suppressed less than 110 W to avoid melting damage of both electrode and substrate.

Fig. 6 shows relationship between MRR and O_2/(O_2+CF_4) ratio of process gas. MRR increased with an increased in O_2/(O_2+CF_4) ratio, and reached maximum value of $1.8x10^{-3}$ mm^3/min when the ratio of O_2 and CF_4 was even. Addition of O_2 is effective because it promotes dissociation of CF_4 for generating fluorine [11], and it also modify SiC to SiO_2 which easily react with fluorine [12].

3.2. Surface morphology

Morphologies of the processed surfaces were evaluated by SWLI and scanning electron microscope (SEM). Fig. 7 shows cross-sectional shape of the removal spot measured by SWLI. Dotted line and solid line show the cross-sectional shape of the removal spot, which were formed with plasma irradiation time of 1 min and 2 min, respectively. Surface roughness became worse with increasing depth of removal spot. Fig. 8 shows the surface morphology of RS-SiC substrates. Fig. 8(a) and (b) show the surface polished by diamond abrasive and the surface irradiated He/CF_4/O_2 plasma with 1 min, respectively. RS-SiC substrate contains α-SiC grain as a raw material, newly synthesized β-SiC grain, and the residual Si [13]. Comparing these two images elucidates that residual silicon was preferentially removed from the surface compared to the SiC grain, and many pores were formed on the surface.

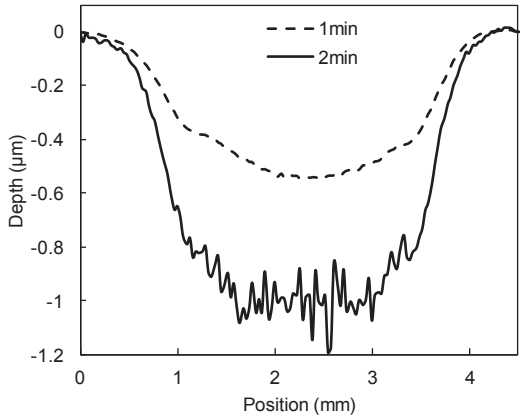

Fig. 7. Cross-sectional shape of the removal spot (Power: 100 W, Flow rate: He:CF_4:O_2=750:5:5 sccm, Gap: 500 μm)

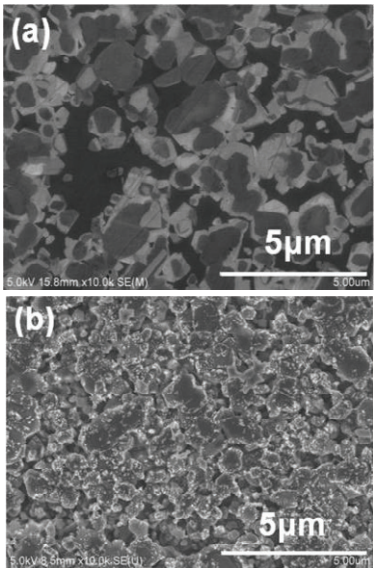

Fig. 8. SEM images of RS-SiC surface (a) Polished surface by diamond abrasive. (b) Etched surface by 1 min plasma irradiation

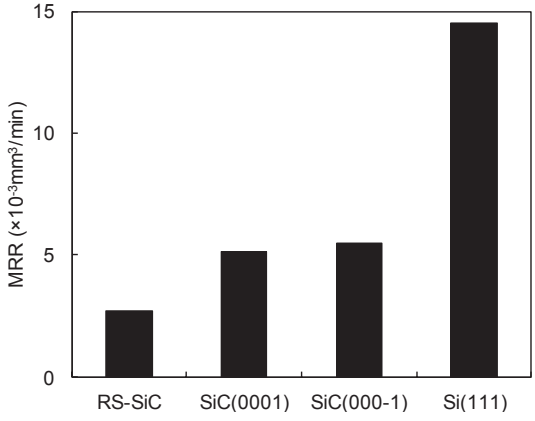

Fig. 9. Comparison of MRR in same etching conditions (Power: 100 W, Flow rate: He:CF_4:O_2=750:5:5 sccm, Gap: 500 μm)

To investigate the differences of removal rate between SiC and Si, etching experiments were conducted for RS-SiC, single crystal SiC (4H-SiC(0001),(000-1), ρ=0.1 Ωcm), and single crystal Si (SiC(111), ρ=0.5 Ωcm) substrates using same processing parameters. Fig. 9 shows comparison of MRR in RS-SiC, 4H-SiC(0001), 4H-SiC(000-1), and Si(111). These results indicate that MRR of Si(111) is about 3 times greater than that of SiC, and MRR of SiC(0001) and SiC(000-1) are almost the same. These results lead to the conclusion that difference of MRR between SiC and Si caused degradation of the surface roughness of the RS-SiC substrate.

4. Summary

In this paper, we demonstrated removal properties of RS-SiC substrate by open-air type PCVM machine using He based CF_4/O_2 mixture process gas. Size of the removal spot and linearity of the relationship between removal volume and plasma irradiation time were sufficient for numerically controlled figuring with a spatial resolution of millimetre level. However, surface roughness increased with an increase in removal depth. RS-SiC consists of α-SiC grain, newly synthesized β-SiC grain, and the residual Si. Removal rate of Si was 3 times greater than that of SiC. It is concluded that inhomogeneous removal of RS-SiC component resulted in degradation of the surface roughness by forming pores. Therefore, optimization of process parameters, such as composition of process gas, is essential to obtain high-integrity surface.

Acknowledgements

This work was partially supported by Adaptable and Seamless Technology Transfer Program through Target-driven R&D, JST.

References

[1] Suyama, S., Kameda, T., Itoh, Y., 2003. Development of high-strength reaction sintered silicon carbide, Diamond and Related Materials 12, p. 1201.
[2] Zhou, L., Audurier, V., Pirouz, P., 1997. Chemomechanical Polishing of Silicon Carbide, J. Electrochem. Soc. 144, p. L161.
[3] Lee, H. S, Jeong, H. D, 2009. Chemical and Mechanical Balance in Polishing of Electronic Materials for Defect-Free Surfaces, Annals of the CIRP 58, p. 485.
[4] Lee, H.S., Kim, D.I., An, J.H., Lee, H.J., Kim, K.H., Jeong, H., 2010. Hybrid Polishing Mechanism of Single Crystal SiC Using Mixed Abrasive Slurry (MAS), Annals of the CIRP 59, p.333.
[5] Mori, Y., Yamauchi, K., Yamamura, K., Sano, Y., 2000. Development of plasma chemical vaporization machining, Rev. Sci. Instrum. 71, p. 4627.
[6] Yamamura, K., Shimada, S., Mori, Y., 2008. Damage-free improvement of thickness uniformity of quartz crystal wafer by

plasma chemical vaporization machining, Annals of the CIRP 57, p. 567.
[7] Yamamura, K., Takiguchi, T., Ueda, M., Hattori, A. N., Zettsu, N., 2010. High-integrity finishing of 4H-SiC (0001) by plasma-assisted polishing, Adv. Mater. Res. 126-128, p. 423.
[8] Yamamura, K., Takiguchi T., Ueda, M., Deng, H., Hattori, A.N., Zettsu, N., 2011. Plasma Assisted Polishing of Single Crystal SiC for Obtaining Atomically Flat Strain-Free Surface, Annals of the CIRP 60, p. 571.
[9] Yamamura, K., Ueda, M., Takiguchi,T., Zettsu, N., 2010. Plasma Assisted Polishing of Reaction-Sintered Silicon Carbide, 25th Annual Meeting of the ASPE, p. 61.
[10] Yamamura, K., Ueda, M., Deng, H., Zettsu, N., 2011. High-integrity finishing of reaction sintered SiC by plasma assisted polishing using ceria abrasive, 11th International Conference of the European Society for Precision Engineering and Nanotechnology, p. 422.
[11] Mogab, C.-J., Adams, A.-C., Flamm, D.-L., 1978. Plasma Etching of Si and SiO_2 –The Effect of Oxygen Additions to CF_4 Plasmas, J. Appl. Phys. 49, p. 3796.
[12] Sano, Y., Watanabe, M. Yamamura, K., Yamauchi, K., Ishida, T., Arima, K., Kubota, A., and Mori, Y., 2006. Polishing characteristics of silicon carbide by plasma chemical vaporization machining, Jpn. J. Appl. Phys. 45, p. 8277.
[13] Suyama, S, Itoh, Y., 2007. Evaluation of microstructure of high-strength reaction-sintered silicon carbide of optical mirror, Proc. of SPIE 6666, p. 66660K-1.